A linear perturbation computation method for hydrodynamic stability studies of complex flows: application to an ICF target implosion

Carine Boudesocque-Dubois, Jean-Marie Clarisse & Jean-Luc Willien

CEA Bruyères le Châtel,
France
carine.boudesocque@cea.fr
jean-marie.clarisse@cea.fr
jean-luc.willien@cea.fr
http://www-dam.cea.fr

Linear hydrodynamic instabilities in inertial confinement fusion (ICF) target implosions have been previously investigated using linear perturbation codes (*e.g.* Henderson *et al.*, 1974; Dufour *et al.* 1984). In the context of direct drive implosions, a simple physical model may be retained which corresponds to that of ideal gas dynamics with electronic heat conduction and a laser energy deposition modeling. The resulting systems of equations which are incompletely parabolic, are here written in Lagrangian coordinates for both the spherical symmetric flow and its linear three-dimensional perturbations. Each one dimensional (1D) system is treated using an operator splitting between a hyperbolic reduced system and a parabolic equation.

The proposed numerical method significantly differs from previous linear perturbation computation methods, which were based on artificial viscosity schemes (Henderson *et al.*, 1974; Grishina, 1980; Dufour *et al.*, 1984), in that it relies on a finite-volume formulation and explicit Godunov-type schemes (Clarisse *et al.*, 2004) for the hyperbolic reduced systems. The complementary nonlinear/linear parabolic equations are classically handled using semi-implicit iterative/direct methods. Despite the additional difficulties raised by the linear perturbation computations of the symmetric flow discontinuities (*i.e.*, shock-waves), the present numerical method is both reliable and fairly accurate and, above all, is less expensive than 2D-numerical methods by, at least, two orders of magnitude, given the spatially grid coarseness commonly advised for hydrodynamic instability calculations (Holmes *et al.*, 1999). This last feature may be profitably used to obtain detailed descriptions of linear perturbation evolutions during ICF target implosions, as illustrated bellow. The above described numerical methods are currently implemented in a linear perturbation code, SILE$\mathcal{X}$, dedicated mainly to ICF applications.

As an illustration of the capabilities of the proposed numerical methods, we show, in the following, results obtained for a *Laser MégaJoule* direct-drive designed target (X. Fortin *et al.*, 1999). For this particular target, it turns out that a sufficiently accurate description of the mean flow requires the use of a 1D grid with at least $3\,10^3$ points (10^3 in each of the ablator, iced DT and gaseous DT layers). Thanks to the numerical method, numerical diffusion is small, and, in particular, shock-shock interactions are sharply described (see silde 13). Linear perturbation results were obtained for a wide range of spherical harmonic degrees ($\ell = 4$, 8, 16, 128, 256, 512, 768). For each linear perturbation computation, the spatial grid was adapted to ensure initially a minimum of at least 100 grid points per local wave length ($\approx 2\pi r/\ell$) down to one half the radius of the gaseous DT central layer. For example, this criterion resulted into the use of a 1D grid of 12146 points for the

treatment of the harmonic degree $\ell = 768$. Space-time evolutions of the target radius perturbations are presented for $\ell = 16$ and $\ell = 128$. Comparing results obtained for $\ell = 16$ and $\ell = 128$ in the ablator, we note that radius perturbation amplitude is smaller upstream the ablation zone than downstream for small ℓ-values while the opposite is true for large ℓs. The evolution of the radius perturbation in the compressed ablator and iced DT layers can be decomposed into two stages: *(i)* from the beginning of the shell irradiation up to the iced/gaseous DT interface-first shock front interaction and *(ii)* from this interaction up to the end of the computation. During the first stage, spatial structures appear on the radius perturbation with a characteristic length which decreases with ℓ. During the second stage, perturbation amplitude increases rapidly and uniformly, and time oscillations appear at the iced/gaseous DT interface. The same kind of spatial structures as observed in the iced DT layer during stage *(i)* appears dowstream of the shock wave as it converges in the gaseous DT core. These fine scale structures are only visible for sufficiently dense spatial grids, hence the importance of 1D grid refinements near the center of the target. To our knowledge, such fine details of implosion flows have never been exhibited by multi-D simulations.

References

Clarisse, J.-M., Jaouen, S., and Raviart, P.-A. 2004 A Godunov-type method in Lagrangian coordinates for computing linearly-perturbed planar-symmetric flows of gas dynamics; *J. Comput. Phys.* **198**.

Dufour, J.-M., Galmiche, D., and Sitt, B. 1984 Investigation of hydrodynamic stability of high aspect ratio targets in laser implosion experiments; in *Laser Interaction and Related Plasma Phenomena*, Plenum Publishing Corp., 709.

Fortin, X., Canaud, B. 1999 Direct drive laser fusion calculations at CEA; in *IFSA*, Elsevier, 102.

Grishina, G.A. 1980 Linear approximation method in gas dynamics problem numerical computations; *USSR Academy of Sciences IAM*, preprint 121, Moscow.

Henderson, D.B., McCrory, R.L., and Morse, R.L. 1974 Ablation stability of laser-driven implosions; *Phys. Rev. Let.*, **33**:4.

Holmes, R.L., Dimonte, G., Fryxell, B., Gittings, M.L., Grove, J.W., Schneider, M., Sharp, D.H., Velikovich, A.L., Weaver, R.P., Zhang, Q. 1999 Richtmyer-Meshkov instability growth: experiment, simulation and theory; *J. Fluid Mech.* **389**.

9th International Workshop on the Physics of Compressible Turbulent Mixing, 19-23 July 2004

A Linear Perturbation Computation Method for Hydrodynamic Stability Studies of Complex Flows: Application to an ICF Target Implosion

C. Boudesocque-Dubois, J.-M. Clarisse and J.-L. Willien

carine.boudesocque@cea.fr, jean-marie.clarisse@cea.fr, jean-luc.willien@cea.fr

CEA Bruyères le Châtel - B.P.12
91680 Bruyères le Châtel - France

Physical Modeling:

Usual hypotheses in ICF hydrodynamics:

- ✗ inviscid and immiscible fluids;
- ✗ one-dimensional mean flow.

Additional hypotheses:

- ✓ single temperature ($T_i = T_e$);
- ✓ non linear heat conduction with fluids conductivities of the form:

$$\kappa = \chi \rho^{-m} T^n, \quad m \in \mathbb{R}, n \in \mathbb{R}^+;$$

- ✓ laser energy deposition modeling at critical density;

✓ Analytical equations of state

- ➥ perfect gas
- ➥ stiffened gas

$$p = P(\rho,T) = \underbrace{\rho(\gamma-1)\mathsf{C_v}T}_{\text{perfect gas}} + p_K(\rho),$$

$$\mathcal{E} = E(\rho,T) = \overbrace{\mathsf{C_v}T}^{\text{perfect gas}} + \mathcal{E}_K(\rho),$$

with :

$$\mathcal{E}_K(\rho) = \mathcal{E}_0 + \frac{A}{\rho}\left(1 + \frac{1}{\gamma-1}\left(\frac{\rho}{\rho_0}\right)^{\gamma}\right) - \mathsf{C_v}T_0\left(\frac{\rho}{\rho_0}\right)^{\gamma-1} - \frac{A}{\rho_0}\frac{\gamma}{\gamma-1}$$

and

$$p_K(\rho) = \rho^2 \frac{\mathrm{d}}{\mathrm{d}\rho}\mathcal{E}_K(\rho).$$

Problem formulation

- ✎ Flow decomposition =

  planar or spherically symmetric mean flow + perturbations;

- ✎ Lagrangian description of mean flow and perturbations;
- ✎ Linear approximation of perturbations;
- ✎ Helmholtz decomposition of the transverse perturbation motion;
- ✎ Fourier or spherical harmonics decomposition of perturbations in the transverse directions;
- ✎ Initial and boundary value problems for:
  - mean flow ($\mathcal{P}$) ;
  - linear perturbation modal (Fourier or spherical harmonics) components ($\widetilde{\mathcal{P}}$).

Notations - Planar or spherical symmetry

symmetry	planar	spherical
symmetry exponent s	0	2
mean flow metric coordinate λ	x	r
$\mathcal{A} = \lambda^s$	1	r^2
Lagrangian coordinate η : $d\eta = \rho \mathcal{A} d\lambda$	$d\eta = \rho dx$	$d\eta = \rho r^2 dr$
modal component characteristic number w	$-{k_\perp}^2$	$-\ell(\ell+1)$
$\widetilde{\mathcal{A}} = s\lambda^{(s-1)}\widetilde{\lambda}$	0	$2r\widetilde{r}$

(area)

Mean flow: system of equations

$$\begin{cases} \dfrac{\partial \mathbf{U}}{\partial t} + \dfrac{\partial}{\partial \eta}\left\{\mathbf{f}_H + \mathbf{f}_P\right\} = \mathbf{S_H}\,, \\ \dfrac{\partial \lambda}{\partial t} = v_\lambda\,, \end{cases} \qquad (\mathcal{S})$$

with:

the conservative variable vector

$$\mathbf{U} = \begin{pmatrix} \tau \\ v_\lambda \\ e \end{pmatrix},$$

the conservative variable flux vector

$$\mathbf{f}_H = \begin{pmatrix} -v_\lambda \\ p \\ p\, v_\lambda \end{pmatrix},$$

the symmetry term $\mathbf{S_H} = \begin{pmatrix} 0 \\ p\,\dfrac{\partial \mathcal{A}}{\partial \eta} \\ 0 \end{pmatrix}$,

the heat conduction flux vector,

$$\mathbf{f}_P = \begin{pmatrix} 0 \\ 0 \\ \Psi_\lambda \end{pmatrix},$$

where $\Psi_\lambda = -\rho\,\kappa\,\dfrac{\partial T}{\partial \eta}$.

Linear perturbation modal components: system of equations

$$\begin{cases} \dfrac{\partial \widetilde{\mathbf{U}}}{\partial t} + \dfrac{\partial}{\partial \eta}\left\{\mathcal{A}\left(\widetilde{\mathbf{f}_H} + \widetilde{\mathbf{f}_P}\right) + \widetilde{\mathcal{A}}\left(\mathbf{f}_H + \mathbf{f}_P\right)\right\} + \dfrac{\partial}{\partial \eta}\left\{\mathcal{A}\left(\mathbf{f}_H + \mathbf{f}_P\right)\right\}\widetilde{\Theta} \\ \qquad\qquad = \widetilde{\mathbf{S_H}} + \mathbf{S_H}\,\widetilde{\Theta} + \mathbf{R}_H\,\widetilde{\Omega} + \widetilde{\mathbf{Q}_P}\,, \\ \dfrac{\partial \widetilde{\lambda}}{\partial t} = \widetilde{v}_\lambda, \qquad \dfrac{\partial \widetilde{\Theta}}{\partial t} = \widetilde{\Omega}, \qquad \dfrac{\partial}{\partial t}\left(\mathcal{A}\widetilde{\Omega}\right) = w\left(\mathcal{A}\,\dfrac{\partial p}{\partial \eta}\,\widetilde{\lambda} - \tau\,\widetilde{p}\right), \end{cases} \qquad (\widetilde{\mathcal{S}})$$

with:

- $\widetilde{\mathbf{U}}$ the conservative-variable linear perturbation vector,
- $\widetilde{\mathbf{f}_H}$ the 1D conservative-variable linear perturbation flux vector, $\widetilde{\mathbf{f}_H} = (\partial \mathbf{f}_H/\partial \mathbf{U})\,\widetilde{\mathbf{U}}$,
- $\widetilde{\Theta}$ the transverse-motion linear perturbation dilatation,
- $\widetilde{\Omega}$ the transverse-motion linear perturbation expansion,
- $\mathbf{R}_H\widetilde{\Omega}$ the transverse direction conservative-variable linear perturbation flux vector,
- $\widetilde{\mathbf{f}_P}$ the 1D heat-conduction linear perturbation flux vector,
- $\widetilde{\mathbf{Q}_P}$ the transverse direction heat-conduction linear perturbation flux vector,
- $\widetilde{\mathbf{S_H}}$ the linear perturbation symmetry term,

$$\mathbf{R}_H = \tau \begin{pmatrix} 1 \\ 0 \\ -p \end{pmatrix},$$

$$\widetilde{\mathbf{Q}_P} = \begin{pmatrix} 0 \\ 0 \\ w\,\dfrac{\tau}{\mathcal{A}}\left(\kappa\,\widetilde{T} + \Psi_\lambda\,\widetilde{\lambda}\right) \end{pmatrix}.$$

Mean flow and perturbations — mathematical aspects

- Systems ($\mathcal{S}$) and ($\widetilde{\mathcal{S}}$) are incompletely parabolic[a] 1D-systems. In effect, ($\mathcal{S}$) and ($\widetilde{\mathcal{S}}$) are decomposed in *(i) hyperbolic reduced systems* ($\mathcal{S}_H$) and ($\widetilde{\mathcal{S}}_H$) in the conservative variable $\mathbf{U}$ and $\widetilde{\mathbf{U}}$ and *(ii) parabolic scalar equations* ($\mathcal{E}_P$) and ($\widetilde{\mathcal{E}}_P$).
- Both ($\widetilde{\mathcal{S}}_H$) and ($\widetilde{\mathcal{E}}_P$) are merely linear systems for perturbations BUT with possibly *discontinuous coefficients*.
- In fact, main difficulty is raised by the linear perturbation hyperbolic system ($\widetilde{\mathcal{S}}_H$). Any discontinuity of the flux-function $\mathbf{f}_H$ (shock wave of the mean flow) will result in a Dirac mass[bc] for the modal component solution of ($\widetilde{\mathcal{S}}_H$).
- One can only expect *weak convergence* of the modal components.

> ➽ Specific methods are required for the numerical approximation of such hyperbolic systems.

[a] B. Gustafsson *SIAM J. Appl. Math.* 1978.
[b] G. A. Grishina *USSR Academy of Sciences IAM* 1980.
[c] E. Godlewski and P.-A. Raviart *Math. Comput. Simulation* 1999.

Mean flow and perturbations — numerical methods

- 2 or 3 stage splitting method [a] between hyperbolic systems ($\mathcal{S}_H$ and $\widetilde{\mathcal{S}}_H$) and parabolic equations ($\mathcal{E}_P$ and $\widetilde{\mathcal{E}}_P$).

Numerical method — hyperbolic problems

Earlier linear perturbation computation methods were based on artificial viscosity schemes[bc]. Because of the weak convergence, linear perturbation numerical results may be extremely noisy and therefore useless for linear stability analyses. Note that this defect can also arise in 2D/3D hydrodynamic instability simulations in the small amplitude regime. The key points in devising linear perturbation computational methods are:

- a mean flow computational method capable of producing accurate results without oscillations in smooth parts of the flow.
- a scheme for the linear perturbations which reflects the properties (hyperbolicity) of the linear perturbation hyperbolic system $\widetilde{\mathcal{S}}_H$. Such a scheme will introduce needed dissipation at mean flow discontinuities (shock wave) and little or no dissipation in smooth parts of this flow.

ov type schemes are the best candidates for the 1^{st} point and can be extended to fulfill the 2^{nd} point.

[a] G. Strang *SIAM J. Numer. Anal.* 1968
[b] G. A. Grishina *USSR Academy of Sciences IAM* 1980.
[c] D.B. Henderson, R.L. McCrory and R.L. Morse *Phys. Rev. Let.* 1974.

Numerical method — hyperbolic problems

Integration of hyperbolic problems $\mathcal{P}_H$ and $\widetilde{\mathcal{P}}_H$:

- finite-volume formulation;
- explicit Godunov-type scheme [a] using an acoustic solver and its linearization. The principles involved in the linearization of the gas dynamics solver are immediately applicable to more sophisticated fluid models with zero entropy flux such as 2 temperature plasmas, 3 temperature radiative hydrodynamics, magnetohydrodynamics, elastoplasticity, ...
- half-Riemann problem approach for time-dependent boundary conditions;
- explicit 3 step Runge-Kutta time integrator [b];
- time step constraint for numerical stability:

$$\Delta t \quad = \quad \underbrace{\frac{\Delta\lambda}{c}}_{\text{1D-CFL}} \quad / \quad \underbrace{\mathcal{F}\left(\frac{w}{\mathcal{A}}\Delta\lambda^2\right)}_{\text{modal component weight}}$$

where $\mathcal{F}\left(\frac{w}{\mathcal{A}}\Delta\lambda^2\right) \underset{w\Delta\lambda^2/\mathcal{A}\gg 1}{=} O\left(\sqrt{\frac{w}{\mathcal{A}}\Delta\lambda^2}\right)$.

[a] J.-M. Clarisse, S. Jaouen and P.-A. Raviart *J. Comp. Phys.* 2004

[b] C.-W. Shu and S. Osher *J. Comp. Phys.* 1988

Numerical method — parabolic problems

Integration of parabolic problems $\mathcal{P}_P$ and $\widetilde{\mathcal{P}}_P$:

- finite-difference discretisation;
- implicit scheme (θ-scheme);
- iterative method for $\mathcal{P}_P$;
- direct method for $\widetilde{\mathcal{P}}_P$;
- time-dependent boundary conditions.

Numerical methods — SILEX code

These numerical methods are currently available in the linear perturbation code SILEX.

Linear perturbation computation method

Features of the proposed method:

- ✎ Reduced computational cost (2 orders of magnitude) compared to 2D/3D computations;
- ✎ Numerical experiments[a] show that the number of points per wave length $N = \frac{2\pi}{\Delta\lambda}\sqrt{\frac{\mathcal{A}}{w}}$ should be $\gtrapprox 100$ in order to obtain reasonably accurate results[b];
- ✎ Tested against various configurations:
  - ⇝ rippled shock problem[c];
  - ⇝ Richtmyer-Meshkov instability computations[a];
- ✎ Study of a self-similar planar ablation flow[d].
- ✎ Current applications:
  - ➢ Radiation induced Richtmyer-Meshkov instability[e].
  - ➢ ICF direct drive target implosion (see below).

[a] J.-M. Clarisse, S. Jaouen and P.-A. Raviart *J. Comp. Phys.* 2004.
[b] G. A. Grishina *USSR Academy of Sciences IAM* 1980, a value of $N \approx 10\pi$ is advised.
[c] S. Jaouen, thesis 2001.
[d] C. Boudesocque-Dubois and J.-M. Clarisse *ECLIM* 2002.
[e] M. Legrand and J.-M. Clarisse, *this conference*.

Numerical computations – LMJ target[a]

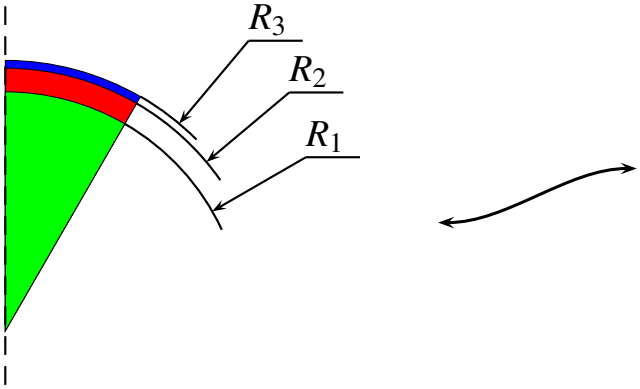

equation of state

$[R_2, R_3]$	CH	stiffened gas
$[R_1, R_2]$	DT (cryogenic)	stiffened gas
$[0, R_1]$	DT (gas)	perfect gas

electronic heat conduction

$(m = 0, n = 5/2)$

– Direct drive

Laser energy deposition modeling at critical density

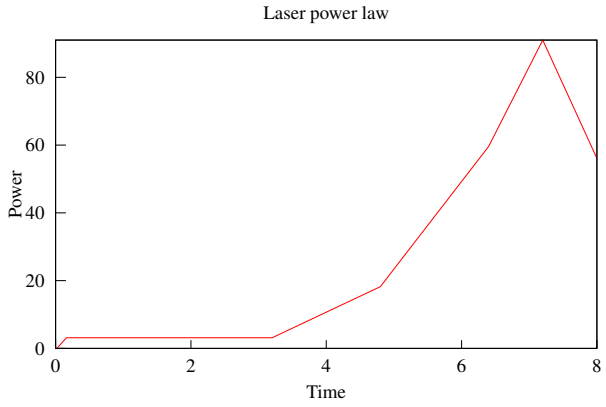

[a] B. Canaud ans X. Fortin *IFSA* 1999
Cambridge, UK

Mean flow

Initial condition $\Longleftrightarrow$ equilibrium state

uniform pressure,

uniform fluid temperature.

Boundary condition

constant pressure.

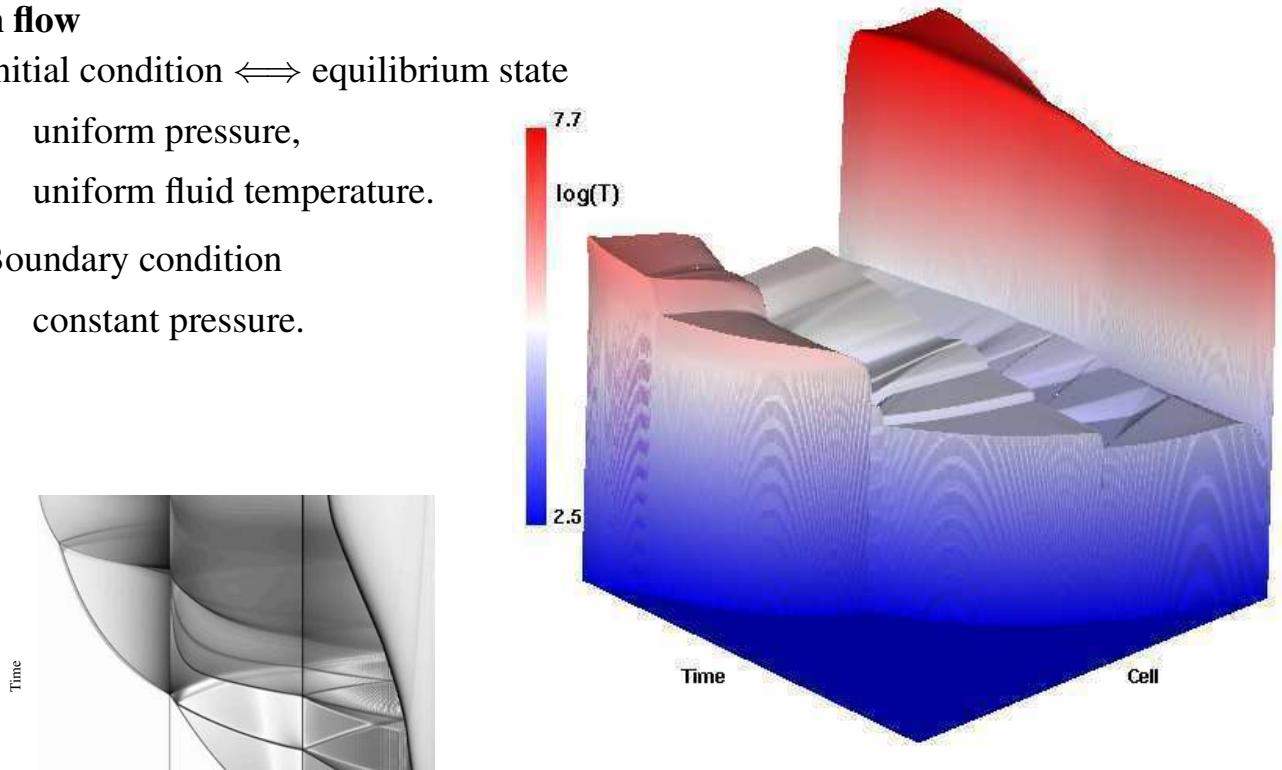

CH	1000	cells
DT (cryogenic)	1000	cells
DT (gas)	1000	cells

Perturbed flow

Initial perturbation

Modal boundary condition

0 pressure,

0 heat flux.

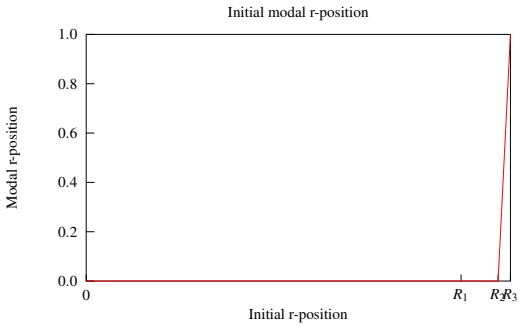

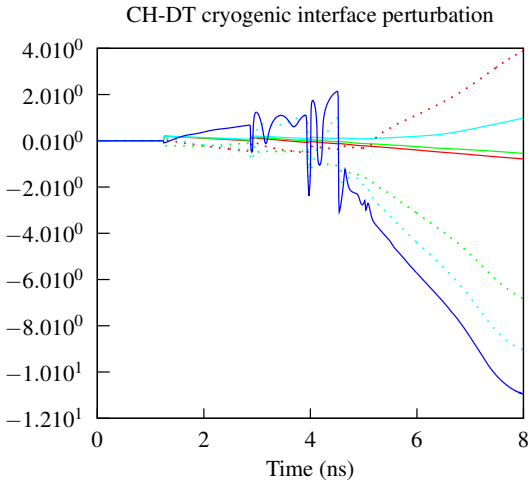

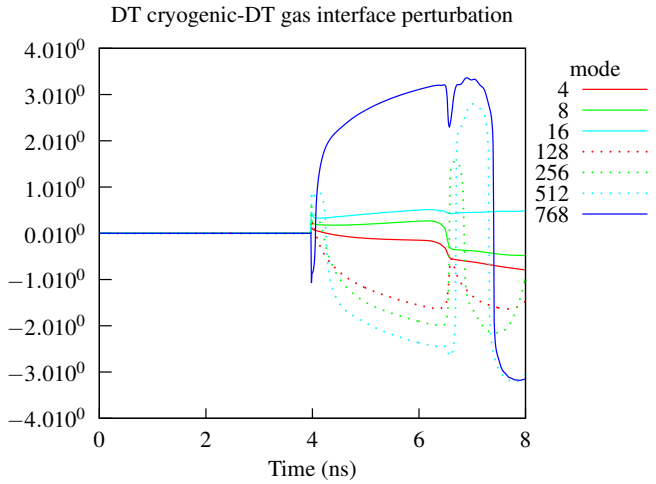

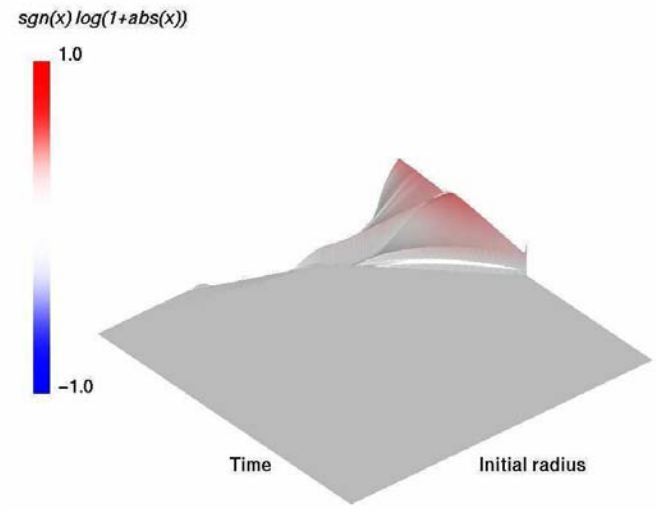

Mode 16
Radius perturbation in DT(gas)

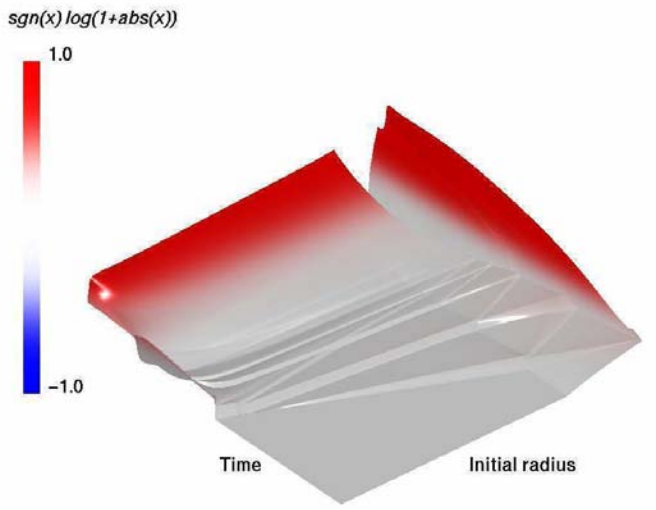

Mode 16
Radius perturbation in DT(cryo) and CH

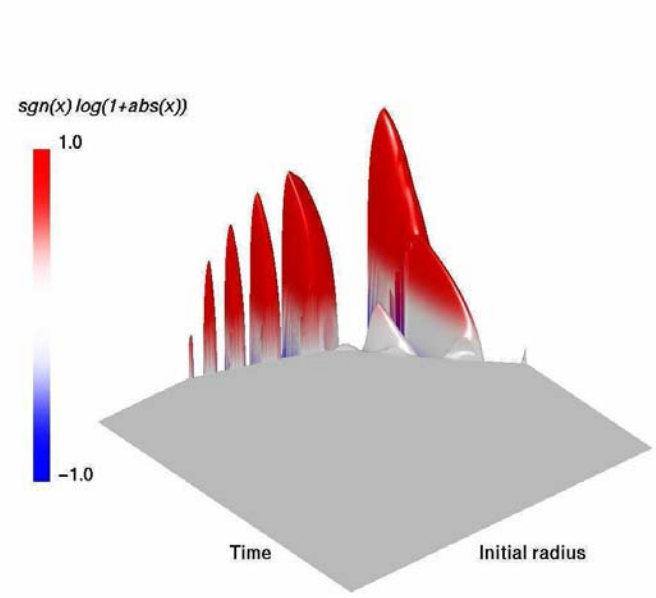

Mode 128
Radius perturbation in DT(gas)

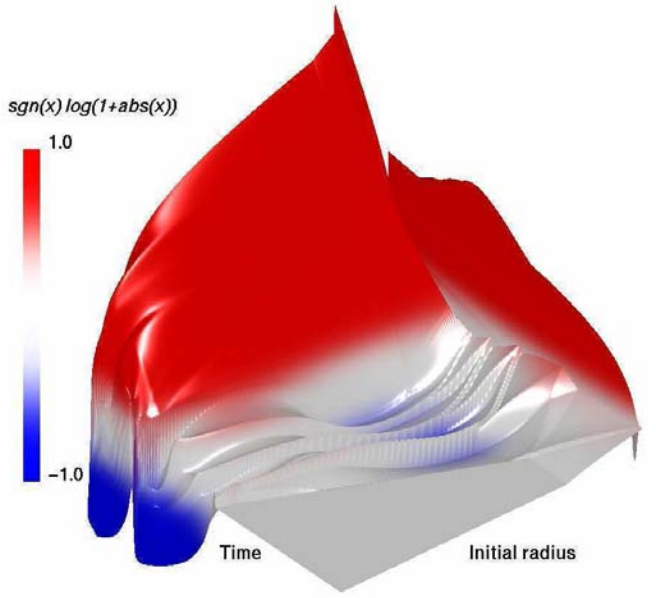

Mode 128
Radius perturbation in DT(cryo) and CH

Prospects

- Application to other "exotic" hydrodynamics instabilities.
- Introduce more sophisticated physical fluid models: 3 temperature radiative hydrodynamics.
- ...